

An MMI-based wavelength combiner employing non-uniform refractive index distribution

Singh, S.; Kojima, K.; Koike-Akino, T.; Wang, B.; Parsons, K.; Nishikawa, S.; Yagyu, E.

TR2014-020 April 2014

Abstract

A novel wavelength combiner using non-uniform refractive index distribution within a multi-mode interference device is proposed and simulated. The refractive index step creates separate localized modes with different effective refractive indices and two modes are strongly excited which form the basis of an interferometer. We applied the concept to 1.30/1.31 μm and 1.31/1.55 μm wavelength combiners on an InP substrate. The lengths of the devices are 1272 μm and 484 μm with simulated insertion losses of 0.6 dB and 0.67 dB respectively.

Optics Express

This work may not be copied or reproduced in whole or in part for any commercial purpose. Permission to copy in whole or in part without payment of fee is granted for nonprofit educational and research purposes provided that all such whole or partial copies include the following: a notice that such copying is by permission of Mitsubishi Electric Research Laboratories, Inc.; an acknowledgment of the authors and individual contributions to the work; and all applicable portions of the copyright notice. Copying, reproduction, or republishing for any other purpose shall require a license with payment of fee to Mitsubishi Electric Research Laboratories, Inc. All rights reserved.

An MMI-based wavelength combiner employing non-uniform refractive index distribution

Siddharth Singh,^{1,2} Keisuke Kojima,^{1,*} Toshiaki Koike-Akino,¹ Bingnan Wang,¹ Kieran Parsons,¹ Satoshi Nishikawa,³ and Eiji Yagyu³

¹Mitsubishi Electric Research Laboratories, 201 Broadway, Cambridge, MA, 02139, USA

²Department of Electrical and Computer Engineering, Stony Brook University, NY, 11794, USA

³Advanced Technology R&D Center, Mitsubishi Electric Corporation, 8-1-1 Tsukaguchi-Honmachi, Amagasaki, Hyogo, Japan

*kojima@merl.com

Abstract: A novel wavelength combiner using non-uniform refractive index distribution within a multimode interference device is proposed and simulated. The refractive index step creates separate localized modes with different effective refractive indices and two modes are strongly excited which form the basis of an interferometer. We applied the concept to 1.30/1.31 μm and 1.31/1.55 μm wavelength combiners on an InP substrate. The lengths of the devices are 1272 μm and 484 μm with simulated insertion losses of 0.6 dB and 0.67 dB, respectively.

© 2014 Optical Society of America

OCIS codes: 230.1360 Beam splitter; 130.7408 Wavelength filtering devices; 230.3120 Integrated optics devices.

References and links

1. Y. Barbarin, X. J. M. Leijtens, E. A. J. M. Bente, C. M. Louzao, J. R. Kooiman, and M. K. Smit, "Extremely Small AWG Demultiplexer Fabricated on InP by Using a Double-Etch Process," *IEEE Photonics Technol. Lett.* **16** (11), 2478–2480 (2004).
2. N. Goto and G. L. Yip, "Y-branch wavelength multi-demultiplexer for $\lambda=1.30 \mu\text{m}$ and $1.55 \mu\text{m}$," *Electron. Lett.* **26**, 102–103 (2007).
3. A. Tervonen, P. Poyhonen, S. Honkanen, and M. Tahkokorpi, "A guided-wave Mach-Zehnder interferometer structure for wavelength multiplexing," *IEEE Photonics Technology Letters* **3**, 516–518 (1991).
4. C. van Dam, M. R. Amersfoort, G. M. ten Kate, F. P. G. M. van Ham, and M. K. Smit, "Novel InP-based phased-array wavelength demultiplexer using a generalized MMI-MZI configuration," *Proc. 7th Eur. Conf on Int. Opt. (ECIO '95)* 275–278 (1995).
5. L.B. Soldano and E.C.M. Pennings, "Optical multi-mode interference devices based on self-imaging: principles and applications," *J. Lightwave Technol.* **13** (4), 615–627 (1995).
6. C. Yao, H.G. Bach, R. Zhang, G. Zhou, J.H. Choi, C. Jiang, and R. Kunkel, "An ultracompact multimode interference wavelength splitter employing asymmetrical multi-section structures," *Optics Express* **20**, 18248–18253 (2012).
7. Y. Shi, S. Anand, and S. He, "A Polarization-insensitive 1310/1550-nm Demultiplexer based on Sandwiched Multimode Interference Waveguides," *IEEE Photonics Technology Letters* **19**, 1789–1791 (2007).
8. M-C. Wu and S-Y. Tseng, "Design and simulation of multimode interference based demultiplexers aided by computer-generated planar holograms," *Optics Express* **18**, 11270–11275 (2010).
9. S. Özbayat, K. Kojima, T. Koike-Akino, B. Wang, K. Parsons, S. Singh, S. Nishikawa, and E. Yagyu, "Application of Numerical Optimization to the Design of InP-based Wavelength Combiners," *Optics Communications* **322**, 131–136 (2014).
10. M. D. Gregory, Z. Bayraktar, and D. H. Werner, "Fast Optimization of electromagnetic design problems using the covariance matrix adaptation evolutionary strategy," *IEEE Trans. Antennas Propagat.* **59** (4), 1275–1285 (2011).

11. D. F. G. Gallagher and T. P. Fellici, "Eigenmode expansion methods for simulation of optical propagation in photonics: pros and cons," Proc. SPIE **4987** 69–82 (2003).
 12. Y. P. Li, C. H. Henry, E. J. Laskowski, H. H. Yaffe, and R. L. Sweatt, "Monolithic optical waveguide 1.31/1.55 μm WDM with -50dB crosstalk over 100 nm bandwidth," Electron. Lett. **31** 2100–2001 (1995).
-

1. Introduction

Wavelength combiners are essential components for wavelength division multiplexing (WDM) optical communications systems. There has been interest in InP-based photonic integrated circuits where multiple lasers, modulators and beam combiners can be monolithically integrated on a single chip for WDM optical communications systems. It is therefore desirable to design wavelength combiners on InP substrates.

Several device concepts have been utilized to realize wavelength combiners such as arrayed waveguide devices (AWG) [1], Y branch devices [2], Mach-Zehnder interferometer (MZI) devices [3, 4] and multimode interference (MMI) devices [5] to name a few important ones.

For general power splitters or combiners, MMI devices are particularly attractive as they offer several advantages such as robust fabrication tolerances, ease of fabrication, compact size and low excess loss. However, MMI-based wavelength combiners which are based on the theory of self-imaging will lead to very long devices especially when combining wavelengths which are 10 nm apart due to the fact that the device length needs to equal several odd and even multiples of the beat lengths for both wavelengths. The conventional theory of MMI devices requires that for an MMI device to split two wavelengths λ_1 and λ_2 , the length of the device L must satisfy the condition [5],

$$L = M \times L_\pi(\lambda_1) = (M + 1) \times L_\pi(\lambda_2) \quad (1)$$

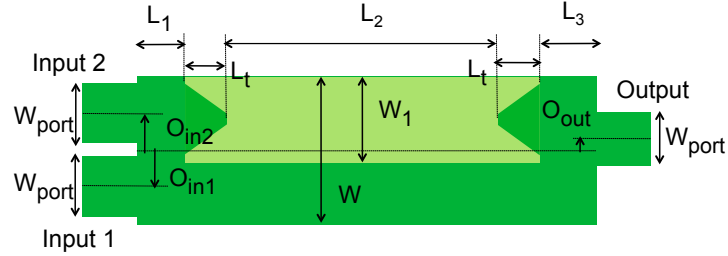
where $L_\pi(\lambda)$ is the wavelength-dependent beat length [5] and M is a positive integer. The beat length for an MMI device of width W can be approximated by $L_\pi = 4n_{eff}W^2/3\lambda$. For 10 nm wavelength spacing one can see that with $W = 6\mu\text{m}$, L would be over 10 mm long. Although novel MMI-based wavelength combiners have been proposed for InGaAsP/InP and silicon-on-insulator (SOI), they have typically targeted very large wavelength spacings of 240 nm such as 1.31/1.55 μm where it is much easier to design shorter devices [6, 7, 8].

Recently, we proposed to use up to sixteen pieces of relatively small patches of different refractive index within MMI, and used a computer optimization algorithm to design efficient two beam and four beam wavelength combiners [9]. One important finding of the paper was that computer algorithms can optimize the device structure with tens of parameters with good performance. By closely looking at the beam propagation patterns of the two beam combiner, it was deduced that the collective refractive index pattern acted as an interferometer. So the next logical step would be to build an interferometric wavelength combiner using a few very long enough refractive index steps. In this paper, we propose a novel MMI device concept in which non-uniform refractive index forms two distinct modes and its middle section acts as an interferometer. Unlike typical MZI-based wavelength combiners, this device does not rely on the length difference of two arms, so it can be made as a straight and narrow device. This may be an important feature for many applications. In order to demonstrate that the concept works for a wide range of wavelengths, we designed two types of wavelength combiners, one for 1.30/1.31 μm and another for 1.31/1.55 μm . Although the results presented in this paper are for specific wavelength spacings of 10 nm and 240 nm, combiners for other wavelength spacings can be readily designed using our proposed device concept. Although all our simulation results are based on a wavelength combiner it is straightforward to extend them to act as wavelength splitters with slightly different optimization criteria such as maximizing the extinction ratio.

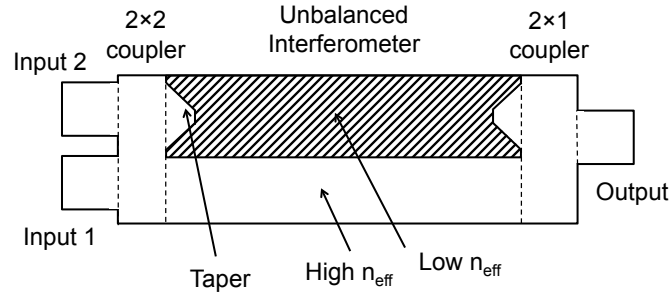
2. Principle and design

The top view of the proposed device is shown in Fig. 1(a), where the lighter green part shows the lower refractive index region, and the rest constitute the higher refractive index regions.

The functional diagram of the proposed device is depicted in Fig. 1(b) and it can be divided into three sections. The 2×2 coupler (leftmost section) splits the input field into two, and excites the two main modes in the unbalanced interferometer section, whose detail will be explained later. The outputs of the unbalanced interferometer are combined into the output port by a 2×1 coupler. The taper sections smoothly guides the modes with different waveguide heights.



(a) Schematic view with dimensions.



(b) Functional diagram.

Fig. 1: Top view of the proposed device.

The cross-sectional view of the interferometer section is shown in Fig. 2. An $\text{In}_{1-x}\text{Ga}_x\text{As}_{1-y}\text{P}_y$ ($y = 0.4$) core layer sandwiched between an InP substrate and InP cladding layer. The core layer is etched by a small constant thickness T_g at a pre-determined rectangular plus taper shape creating a groove. In order to precisely control T_g , it is possible to insert a thin etch-stop layer which has different $\text{In}_{1-x}\text{Ga}_x\text{As}_{1-y}\text{P}_y$ composition, such as InP. The groove is then filled with an InP regrown layer. This creates nearly-localized propagation modes with distinct effective refractive indices in the MMI, unlike conventional uniform MMIs. Figures 3(a) and 3(b) show the lowest TE mode and the third lowest TE mode respectively, when the total MMI width is $W = 6.0 \mu\text{m}$, the patch width is $W_1 = 3.6 \mu\text{m}$, core layer thickness is $T_{\text{core}} = 0.5 \mu\text{m}$, and groove thickness is $T_g = 0.2 \mu\text{m}$. The effective high and low refractive indices are 3.3001 and 3.2671 respectively at $1.30 \mu\text{m}$ and 3.29554 and 3.26303 at $1.31 \mu\text{m}$.

In order for the combiner to have maximum efficiency, the following relationship needs to

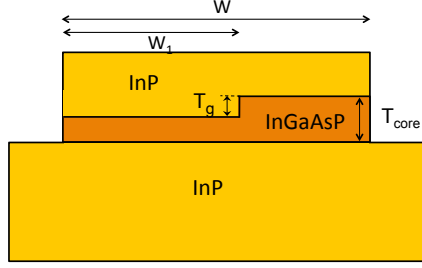


Fig. 2: Cross-sectional view of the center section of the proposed device.

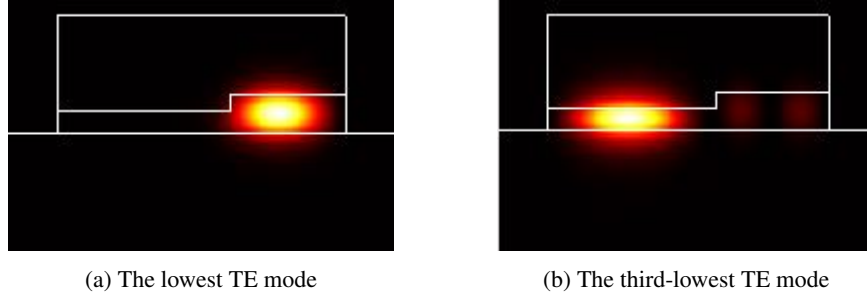


Fig. 3: Mode inside the MMI at the cross-section shown in Fig.2.

hold,

$$\Delta\beta_1 L_0 - \Delta\beta_2 L_0 = \pi \quad (2)$$

where $\Delta\beta_1$ and $\Delta\beta_2$ are the differences in the propagation constant of the two modes at λ_1 and λ_2 respectively, and L_0 is the length of the interferometer section. In our case of 10 nm wavelength difference, L_0 becomes 893 μm .

Since the interferometer is not symmetric in terms of mode positions, instead of using symmetric 2×2 and 2×1 couplers, we use an optimization algorithm to design the asymmetric 2×2 and 2×1 couplers. Multiple parameters were optimized to maximize the output power when λ_1 was injected into input port 1 and the output power when λ_2 was injected into input port 2 [9]. For the optimization algorithm, we used a covariance matrix adaptation evolutionary strategy (CMA-ES) [9, 10]. We optimized widths and offsets of input/output waveguides and the lengths of the 2×2 coupler, unbalanced interferometer, 2×1 coupler and taper sections simultaneously. Considering the fabrication repeatability, the width of the tip of the taper is set to 0.2 μm . In the following two sections, we present simulation results for a 1.30/1.31 μm and 1.31/1.55 μm wavelength combiner.

3. Simulation results - 1.30/1.31 μm wavelength combiner

The proposed device is simulated using the commercial software FIMMWAVE [11] which uses the eigenmode expansion method to solve the propagation problem. A 3-dimensional finite difference mode solver has been employed as a mode solver in all sections. The optimized lengths of the four sections were found to be $L_1 = 197.9 \mu m$, $L_2 = 849.1 \mu m$, $L_3 = 44.9 \mu m$, and $L_t = 89.9 \mu m$. The optimized waveguide widths are $W_{port} = 2.8 \mu m$. The offsets for the input and output ports are $O_{in} = 0.50 \mu m$, $O_{out1} = 1.50 \mu m$ and $O_{out2} = 1.63 \mu m$.

Figures 4(a) and 4(b) show propagation patterns for 1.30 μm input to port 1, and 1.31 μm

input to port 2, respectively. In the interferometer section, two beams are confined into each section. However, since the two modes, as shown in Figs. 3(a) and 3(b), are not totally spatially separated, there are interference patterns as can be seen in the interferometer section. The wavelength-dependent transmission for this device is shown in Fig. 5. Since this device was optimized at $1.30 \mu\text{m}$ and $1.31 \mu\text{m}$, the transmittance (ratio of the output power to the input power) is as high as 0.870 (0.6 dB loss).

We also optimized a device without taper sections. In this case, the transmittance was 0.798, which was 7.2% lower than the case with taper sections. Therefore, taper sections play an important role in guiding beams smoothly between sections with different vertical confinement. Also, the optimized interferometer length was $873.0 \mu\text{m}$, which is close to the optimum length $L_0 = 893 \mu\text{m}$ calculated from Eq.(2). Note that $L_2 = 849.1 \mu\text{m}$ when taper sections are used. So the difference between $873.0 \mu\text{m}$ and $849.1 \mu\text{m}$ shows the effective length of taper section as part of an interferometer. To the best of our knowledge, no attempt has been made at using MMI-based devices for targeting such as a small wavelength spacing to date. The high transmittance achieved using our proposed device concept is promising.

A common device for wavelength splitters or combiners is an AWG. For an InP-based AWG, Barbarin et al. [1] reported very small size of $230 \mu\text{m} \times 330 \mu\text{m}$. On the other hand, our $1.30/1.31 \mu\text{m}$ wavelength combiner has a size of $6 \mu\text{m} \times 1272 \mu\text{m}$. For photonic integrations circuit applications, there may be situations where latter is more favorable than the other.

(a) $1.30 \mu\text{m}$ input to port 1

(b) $1.31 \mu\text{m}$ input to port 2

Fig. 4: Propagation patterns for a $1.30/1.31 \mu\text{m}$ wavelength combiner. The total MMI length is $1271.7 \mu\text{m}$

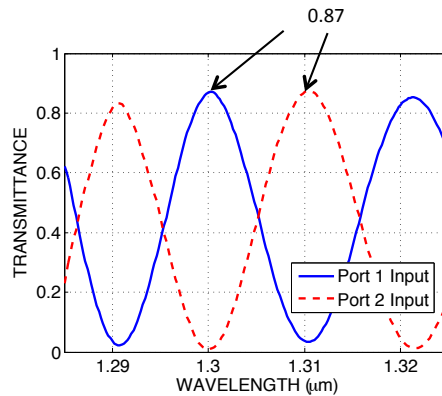


Fig. 5: Wavelength-dependent transmittance of a $1.30/1.31 \mu\text{m}$ wavelength combiner.

4. Simulation results - 1.31/1.55 μm wavelength combiner

Another important application of wavelength combiner is for the 1.31 μm /1.55 μm wavelength spacing. For this application, we re-optimized the device parameters. In this case, MMI width is $W = 8.0 \mu\text{m}$, patch width is $W_1 = 4.5 \mu\text{m}$, input and output waveguide widths of $W_{\text{port}} = 3.0 \mu\text{m}$ were used. We then optimized section lengths and found $L_1 = 253.5 \mu\text{m}$, $L_2 = 11.7 \mu\text{m}$, $L_3 = 52.9 \mu\text{m}$, and $L_t = 83.1 \mu\text{m}$. The offsets for the input and output ports are $O_{\text{in}} = 1.46 \mu\text{m}$, $O_{\text{out1}} = 1.16 \mu\text{m}$ and $O_{\text{out2}} = 2.58 \mu\text{m}$. The total MMI length is $484.3 \mu\text{m}$.

Figures 6(a) and 6(b) show propagation patterns for 1.31 μm input to port 1, and 1.55 μm input to port 2, respectively. These show the effective combining effect clearly. Note that lower refractive index part is on the lower side of the arm.

(a) 1.31 μm input to port 1

(b) 1.55 μm input to port 2

Fig. 6: Propagation patterns for a 1.31/1.55 μm wavelength combiner. The total MMI length is $484.3 \mu\text{m}$.

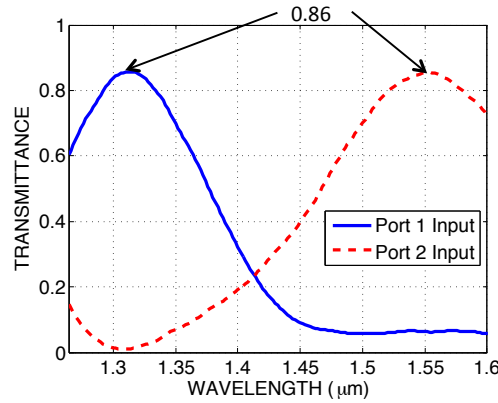
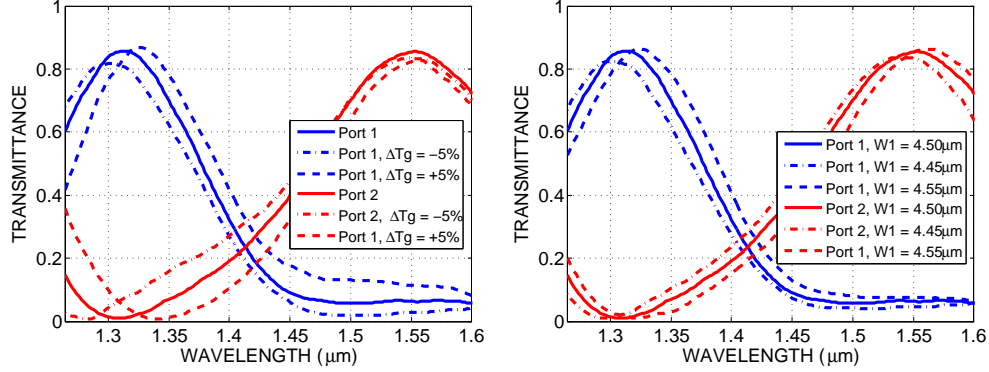


Fig. 7: Transmittance of a 1.31/1.55 μm combiner as a function of wavelength.

The wavelength-dependent transmission for this device is shown in Fig. 7. This device was optimized at 1.31 μm and 1.55 μm and the peak transmittance is as high as 0.856 (0.67 dB loss) which is comparable to the 0.87 transmittance achieved for the 10 nm wavelength spacing. This illustrates the suitability of our device concept for a wide range of wavelength spacings.

In order to evaluate the tolerance to fabrication error, we first changed the groove thickness T_g . Its nominal value is $0.20 \mu\text{m}$ and is changed by $\pm 0.01 \mu\text{m}$ which is 5% deviation from the nominal value. As discussed in Section 2, this can be achieved if we use etch-top layer and selective etching, for example. Figure 8(a) shows that the peak wavelength and height are



(a) Transmittance when T_g is varied.

(b) Transmittance when W_1 is varied.

Fig. 8: Sensitivity analysis of a 1.31/1.55 μm wavelength combiner.

slightly affected. We then calculated the transmittance as a function of wavelength when the groove width W_1 was changed by $\pm 0.05 \mu m$ which can be achieved by the current state-of-the-art lithography and etching technologies. The result is shown in Fig. 8(b), and the device still performs satisfactorily as a 1.31/1.55 μm wavelength combiner. Device optimization technique by taking the fabrication error into account has been discussed in [9], and if we had used this scheme for this device, the device would have been better optimized taking into account such fabrication errors.

The proposed device concept has thus been shown to perform satisfactorily against variations in its groove thickness and width as can be observed by observing the transmittances for varying groove thickness and width in Fig. 8(a) and Fig. 8(b) respectively.

Previous attempt at using InP-based 1.31/1.55 μm MMI wavelength splitters and combiners using had device lengths longer than 960 μm , and simulated insertion loss of about 1.4 dB (worse of the two wavelength) was obtained [6]. So our proposed device is a factor of two improvement in terms of device length. Alternative approach for a 1.31/1.55 μm splitter or a combiner is a cascaded Mach-Zehnder Interferometer made of silica waveguides [12]. This has an excellent performance with fiber-to-fiber insertion loss less than 1dB, and the crosstalk of -50dB. However, the device size is 60 mm \times 0.6 mm.

5. Discussions

With $\lambda = 1.30 \mu m$ input to port 1, the relative power (with input power as 1.0) of the lowest TE mode (the lower arm in Fig. 4(a)) is 0.6171, while that of the third lowest TE mode (the lower arm in Fig. 4(b)) is 0.3125. The other modes have a few percent or less. Therefore, these two modes form the basis for the interferometer. Note that our device was optimized such that the transmittance for $\lambda = 1.30 \mu m$ input to port 1 and $\lambda = 1.31 \mu m$ input to port 2 are maximized simultaneously. If we designed the device as a wavelength splitter, where transmittance for $\lambda = 1.30 \mu m$ input to port 2 and $\lambda = 1.31 \mu m$ input to port 1 are minimized (in reality the device is used in the reverse direction), we would have different device parameters, and more balanced power for the two MMI modes will be obtained. The maximum transmittance in the current design is limited to 0.87. This can be partly explained by observing that the mode shown in 3(b) has a small distribution in the right hand side, and it is not completely spatially separated from lowest TE mode. Hence the interferometer suffers a small loss.

Conventional AWGs or MZIs need to create large path difference (tens of microns, depending

on the wavelength separation), so the device size (area) is typically larger than several hundred square microns. One difference of the proposed MMI-based wavelength combiners over AWGs or MZIs is that they are narrow and straight devices ($W < 10 \mu m$) which can be placed next to each other and will be beneficial when many similar devices need to be integrated on a single chip.

Even though we have focused on the InP material system in this paper, the device concept could readily be extended to other material systems such as SOI by adjusting the effective refractive index within an MMI. The concept of nonuniform refractive index distribution can potentially be extended to $N \times 1$ ($N > 2$) combiner or splitter. For that, one would need to create a structure with modes having multiple (> 2) effective refractive indices by the combination of different core layer thickness and width of the waveguides.

6. Conclusion

A novel device concept for designing compact MMI-based wavelength combiners has been proposed. A refractive index step in the cross-section of the MMI creates two distinct modes, which can be used for an unbalanced interferometer. A wavelength combiner was designed for $1.30/1.31 \mu m$ and $1.31/1.55 \mu m$ as examples. Simulations show that the devices have insertion losses in the range of $0.6 - 0.67$ dB. These devices are significantly shorter than conventional MMI-based wavelength combiners. Since their width is much smaller than conventional AWGs and MZIs, they may have a potential for high density integration on a chip.